Central obesity is selectively associated with cerebral grey matter atrophy in 15 634 subjects in the UK biobank

Running Title Central obesity and brain volumes

Chris-Patrick Pflanz DPhil (1, *), Daniel Tozer PhD (1), Eric L Harshfield PhD (1), Jonathan Tay BSc (1), Sadaf Farooqi MBChB, PhD (2), Hugh S Markus F Med Sci (1)

1 University of Cambridge Stroke Research Group, Neurology Unit, Department of Clinical Neurosciences, Cambridge Biomedical Campus, Cambridge CB2 0QQ, UK.

2 University of Cambridge Metabolic Research Laboratories and NIHR Cambridge Biomedical Research Centre, Welcome Trust-MRC Institute of Metabolic Science, Addenbrooke's Hospital, Cambridge CB2 0QQ, UK.

*Corresponding author:

Chris Patrick Pflanz, BSc MSc DPhil(OXON) AFHEA

University of Cambridge

Department of Clinical Neurosciences

Neurology Unit

Cambridge Biomedical Campus

Cambridge CB2 0QQ

Email: pp474@medschl.cam.ac.uk

Phone: 0044 1223217742

Mobile: 0044 7765307659

Competing Interest Statement The authors have no competing interests to disclose.

Abstract

Background Obesity is a risk factor for both cardiovascular disease and dementia, but the mechanisms underlying this association are not fully understood. We examined associations between obesity, including estimates of central obesity using different modalities, with brain grey matter (GM) volume in the UK Biobank, a large population-based cohort study.

Methods To determine relationships between obesity and the brain we used brain MRI, abdominal MRI, dual-energy X-ray absorptiometry (DXA), and bioelectric whole-body impedance. We determined whether obesity was associated with any change in brain grey matter (GM) and white matter (WM) volumes, and brain network efficiency derived from the structural connectome (wiring of the brain) as determined from diffusion tensor MRI tractography. Using Waist-Hip Ratio (WHR), abdominal MRI and DXA we determined whether any associations were primarily with central rather than peripheral obesity, and whether associations were mediated by known cardiovascular risk factors. We analysed brain MRI data from 15,634.

Results We found that central obesity, was associated with decreased GM volume (anthropometric data: $p = 6.7 \times 10^{-16}$, DXA: $p = 8.3 \times 10^{-81}$, abdominal MRI: $p = 0.0006$). Regional associations were found between central obesity and with specific GM subcortical nuclei (thalamus, caudate, pallidum, nucleus accumbens). In contrast, no associations were found with WM volume or structure, or brain network efficiency. The effects of central obesity on GM volume were not mediated by C-reactive protein or blood pressure, glucose, lipids.

Conclusions Central body fat distribution rather than the overall body-fat percentage is associated with grey matter changes in people with obesity. Further work is required to identify the factors that mediate the association between central obesity and GM atrophy.

Introduction

Obesity is defined as an excess of body fat that adversely effects health and is rising in prevalence globally. It is well recognised that obesity is associated with type-2 diabetes and cardiovascular disease (1). Increasing evidence suggests effects on brain function with links reported between obesity and both cognitive function and dementia (2). Effects on brain structure have been suggested to underlie these associations.

Obesity has been associated with global cerebral grey matter (GM) atrophy (3), but inconsistent associations with white matter (WM) volume have been published with reports of both decreases (4) and increases (5,6). More recent research used diffusion tensor MRI tractography to reconstruct the connectome (characteristic wiring of the human brain at the mesoscale), and derived measures of brain network integrity that essentially indicate the robustness of the connectome against fault. These network metrics have been shown to correlate better with cognition than macrostructural WM volume, or WM hyperintensities (WMH) in both normal ageing (7) and disease states (8) and might be a more sensitive marker of white matter damage in obesity.

Assessing the effect of obesity on the brain is complicated by differing consequences of central or abdominal (high android-to-gynoid ratio which represents an increase in visceral fat around abdominal organs), and peripheral or subcutaneous (low android-to-gynoid ratio) obesity (9,10). The former has been particularly associated with metabolic syndrome (11), type-2 diabetes, myocardial infarction (12), and Alzheimer's disease (13). The effects of central obesity on the central nervous system (CNS) are less well understood.

As precise measurements of body fat and fat distribution are challenging to perform at scale, in clinical practice, anthropometric measures such as BMI (body mass index: weight in kg/height in m^2) and waist-to-hip ratio (WHR) are used. However, abdominal MRI provides a much more reliable assessment of body fat distribution, including the distinction between subcutaneous and visceral fat (14), although unless whole-body MRI is performed this does not allow quantification of total body fat. A further technique, dual-energy X-ray absorptiometry (DXA), can be used to obtain high-precision whole-body scans that provide accurate estimates of the body composition including the three major body components: fat mass, lean tissue mass, and bone mineral mass (15). Whole-body bioelectrical impedance measures also provide indirect estimates of body fat.

To investigate associations between fat mass and fat distribution and the brain we combined the use of brain MRI, abdominal MRI, DXA, and bioelectric whole-body impedance. We determined whether (1) obesity/fat distribution was associated with any change in GM or WM volumes, (2) with impairment of brain network efficiency derived from diffusion-tensor MRI and whether any associations were mediated by cardiovascular risk factors or blood biochemistry markers.

We also determined the relationship between markers of obesity with brain regions including the basal ganglia including caudate, putamen, pallidum and their major output nucleus the thalamus, as well as hippocampal volume as hippocampal atrophy has previously been reported in obesity (16).

Methods

Study participants

UK Biobank is a population-based cohort study comprising ~500 000 men and women aged 40-69 years, recruited across the United Kingdom (England, Scotland, and Wales) between 2006 and 2010 (17). Following an initial assessment, a subset of participants returned for a neuroimaging visit that included brain 3.0T MRI, abdominal 1.5T MRI, and dual-energy X-ray absorptiometry (DXA) an average of 7.7 (SD=1.4) years later. We used data from 15 634 subjects attending this imaging visit in this analysis.

To assess obesity, we used data on BMI and WHR available in all cases, as well as abdominal MRI (N = 15 634), DXA (N = 4 286), and bioelectric whole-body impedance data (N = 15 868). Availability of cognitive scores that were suitable for analysis varied from N = 15 631 for the visual memory and N = 7519 for the trial making task.

UK Biobank received ethical approval from the Research Ethics Committee (reference 11/NW/0382), and all participants provided written informed consent. The present analyses were conducted under UK Biobank application 36509.

Measures of obesity

The following measures of body composition were used, all available as imaging-derived phenotypes in the UK biobank dataset.

(a) BMI and WHR: UK Biobank has an anthropometry category that includes data on manually obtained body composition measure. We used BMI from the

second assessment visit (to correspond to the imaging assessment) and calculated WHR as waist circumference divided by hip circumference.

(b) Whole-body bioelectrical impedance measures that were acquired using the Tanita BC418MA body composition analyser (Tanita Corp., Tokyo, Japan), including segmental estimates of fat mass, fat-free mass.

(c) Abdominal MRI: We used imaging-derived indicators of abdominal composition, namely visceral adipose tissue, abdominal subcutaneous adipose tissue, total adipose tissue volume and total lean tissue volume, derived from abdominal 1.5T-MRI. All abdominal MRI measurements were performed using Siemens 1.5T MAGNETOM Aera (Siemens, Munich, Germany) using two pulse sequences to acquire the data: the first sequence consisted of a single breath-hold cardiac-gated T1-mapping Modified Look-Locker Inversion Recovery (MOLLI) sequence (typically 12 seconds), which acquires a series of seven images (8 mm slice thickness, in-plane pixel spacing 9.3mm) each with a different T-weighting (18). A single transverse slice located at the porta hepatis was chosen to represent the liver. Indices of body composition derived from the abdominal MRI data were supplied by AMRA (Advanced MR Analytics AB, AMRA, Sweden) according to described methods (14,19).

(d) Dual X-ray absorptiometry (DXA): We used imaging-derived phenotypes of body composition, namely android-to-gynoid fat mass ratio, visceral adipose tissue mass, trunk-to-leg fat mass, trunk-to-leg lean mass, fat mass index, and lean body mass index, derived from DXA. DXA data were acquired using an iDXA instrument (GE-Lunar, Madison, Wisconsin) and measures of lean and fat

mass were determined. The iDXA instrument was calibrated to a manufacturer's phantom (GE-Lunar, Madison, Wisconsin) and underwent a daily QC procedure.

Measures of brain structure

Brain MRI scans were acquired on a standard Siemens Skyra 3T (Siemens, Munich, Germany).

Brain volumes and white matter hyperintensities

We used the cerebral GM and WM volumes image-derived phenotypes in the UK Biobank dataset. These were derived from T1-weighted images and analyzed by an image-processing pipeline developed and run on behalf of UK Biobank (18). We used volumes for specific brain regions: the caudate nucleus, putamen, pallidum, thalamus, hippocampus, that were derived from the structural T1-weighted images using FAST (FMRIB's Automated Segmentation Tool) (20).

We analysed the total volume of WM hyperintensities derived by UK Biobank using both T1 and T2-FLAIR images (N = 14 662) and calculated with BIANCA (21).

Diffusion MRI and network construction

We derived network measures from the original diffusion MRI images. Diffusion tensor MRI tractography was used to reconstruct the structural connectome (characteristic wiring of large tracts in the human brain) and brain network metrics were derived from the connectome that are indicative of how robust the brain network is against fault (22).

158 More specifically, diffusion-weighted images were corrected for eddy currents, head
159 motion, outlier slices, and gradient distortion using FSL (FMRIB software library) (23).
160 Diffusion tensors were then fitted using the b = 1 000 s/mm^2 to get fractional anisotropy
161 (FA) images for each subject. Each subjects' FA image was non-linearly registered into
162 standard space (18). The FA image in diffusion space was then used as a seed for
163 deterministic diffusion tractography carried out using MRtrix3 (24). Termination
164 criteria included: 20 mm < streamline length < 250 mm, turning angle > 45°, or voxel
165 FA < 0.15 (25).

166 To construct networks we used the brain regions that are part of the Automated
167 Anatomical Labeling (AAL) atlas (26) to generate adjacency matrices for each subject.
168 These adjacency matrices fully describe the strength of connectivity node by node and
169 represent the connectome at the level of the AAL atlas resolution. This atlas comprises
170 90 manually labelled cortical and subcortical areas (45 per hemisphere) in standard
171 space, after having discarded cerebellar brain regions.

172 The tensorial field calculated from each participant's FA image into standard space was
173 inverted and then applied to the AAL using nearest-neighbor interpolation to register
174 the AAL into diffusion space (where deterministic tractography was carried out). Two
175 areas in the AAL were considered connected if joined by the endpoints of a
176 reconstructed streamline, resulting in a non-zero edge in the adjacency matrix. Edges
177 were weighted according to the number of streamlines connecting two regions,
178 multiplied by the inverse average streamline length, as longer streamlines are seeded
179 multiple times (27). Edges weights < 1 were zeroed to minimize noise-related false
180 positives. This yielded a symmetric, undirected 90×90 adjacency matrix for each
181 subject.

We used the adjacency matrix to compute global and local network efficiencies (28,29), the most commonly used network metrics, using the brain graph package (30) and the igraph package available in R.

Measures of cognitive performance

The cognitive tests used in our study were administered via touchscreen during the MRI visit. Visual memory was assessed using a pairs-matching test and scored as the total number of incorrect matches made. Reaction time was assessed using a timed symbol matching test similar to the card game 'Snap' and scored as the mean response time in milliseconds across all trials containing matching pairs. Prospective memory was assessed by giving participants an instruction they had to remember later in the assessment and scored as 1 if the participant remembered the instruction of their first try or 0 if not. Visual attention and task switching was assessed using a standard Trail Making Test.

Blood biochemistry

Blood samples were collected at recruitment (for all 500 000 participants) and repeat assessment approximately 5 years later (for 20 000 participants), measuring a range of key biochemistry markers (31). Blood glucose, high-density lipoprotein cholesterol, low-density lipoprotein cholesterol and glycated haemoglobin (HbA1c) were drawn from the blood biochemistry assessment at the first visit. The biomarkers were selected for analysis because they represent established risk factors associated with obesity and metabolic syndrome.

Within the UK Biobank study design, two blood pressure measurements were performed using automated or manual devices. We used the manual blood pressure measurement from the first assessment visit for the data analysis described below.

Statistical data analysis

Statistical analyses were carried out using Python's statistical, computing, machine learning packages SciPy (32) and Python's stats package penguin (33)

To investigate the effects of obesity as determined from BMI and WHR measurements, and differentiate the effects of central and peripheral obesity, we stratified participants into 6 groups using previously reported cut-offs (9): 1. Normal weight and no central obesity (males: 18.5 < BMI < 25, WHR < 0.9, females: 18.5 < BMI < 25, WHR < 0.8), 2. Normal weight and central obesity (males: 18.5 < BMI < 25, WHR > 0.9, females: 18.5 > BMI < 25, WHR > 0.8), 3. Overweight and no central obesity (males: 25 < BMI < 30, WHR < 0.9, females: 25 < BMI < 30, WHR < 0.9), 4. Overweight and central obesity (males: 25 < BMI < 30, WHR > 0.8. females: 25 < BMI < 30, WHR > 0.9), 5. General obesity and no central obesity (males: BMI > 30, WHR < 0.9, females: BMI > 30, WHR < 0.8), 6. Both general and central obesity (males: BMI > 30, WHR > 0.9, females: BMI > 30, WHR > 0.80. Subjects who were markedly underweight which may represent cachexia due to another cause (i.e. had a BMI < 18.5) were excluded.

We determined differences between groups for the brain measures: total brain volume (normalized for head size, from T1 images), cerebral GM volume (normalized for head size), WM volume (normalized for head size), log-transformed WM hyperintensities

(normalized for head size), normalized network metrics, and cognitive scores. Analysis of covariance was used to test for group differences in neuroimaging outcomes across the stratified BMI/WHR groups using the following covariates sex, age, Townsend-Deprivation index (TDI), alcohol intake, current smoking, diabetes mellitus, systolic blood pressure, diastolic blood pressure and glycated haemoglobin (HbA1c). Partial correlations were used to test for associations between continuous indicators of obesity and neuroimaging outcomes after adjusting for the same set of covariates.

We also conducted a region-of-interest (ROI) analysis on regional brain volumes, derived from T1 images (see above). Due to previous data implicating basal ganglia circuits and the hippocampus in obesity we studied the following brain regions: caudate, putamen, pallidum, as well as the thalamus, amygdala, nucleus accumbens, and hippocampus. Basal ganglia dysfunction (34) and alterations in amygdala and thalamus (35) and hippocampal volumes (16) have been reported in obesity. The nucleus accumbens plays a role in food addiction (36) and is a target for deep brain stimulation in severe obesity (37).

In a second analysis, anthropometric data (BMI and WHR), impedance measures of body fat and lean body mass, and imaging (abdominal MRI and DXA scans) derived measures of general and central obesity were used as continuous predictors to investigate their effect on the normalized cerebral GM volume using the same covariates as mentioned above. We then determined whether indicators from blood biochemistry or blood pressure mediated the effect of obesity on the normalized GM volume, by running a mediation analysis using IBM SPSS Amos for Structural Equation Modelling (38).

252

253

Results

Sample size

Subjects were included in the data analysis if imaging outcomes and data of the following co-variates were available: sex, age, TDI, alcohol intake, current smoking, diabetes mellitus, systolic blood pressure, diastolic blood pressure and HbA1c.

Data were available for the following number of subjects: Brain volumes N = 15 634; multimodal WMH (based on FLAIR and T1 images) N = 14 662; DTI and network analysis: 14 368. BMI and WHR were available for all subjects who underwent brain imaging. Data on assessment of obesity was available for bioelectric impedance analysis N = 15 437; abdominal MRI N = 5 155; DXA N = 4 212.

BMI, WHR and brain measures

Unless otherwise stated results are adjusted for the covariates (see methods section). There was a significant progressive reduction in cerebral GM volume as WHR increased, with WHR rather than BMI being the primary driver of this association, with GM volume being lowest in people with overweight and central obesity ($p = 6.7\times10^{-16}$, $\eta_p^2 = 0.004$, see Fig 1). The association of combined BMI/WHR group and GM volume appeared to be related to a loss of normalized brain volume ($p = 2.2\times10^{-16}$, $\eta_p^2 = 0.011$). In contrast, there was no association with WM volume ($p = 0.135$, $\eta_p^2 = 0.001$). Furthermore, there was no overall effect of combined BMI/WHR group with any brain network measure: weighted global efficiency ($p = 0.594$, $\eta_p^2 = 0.001$, see Fig 1), weighted local efficiency ($p = 0.607$, $\eta_p^2 = 0.001$). There was a weak association with WM hyperintensities ($p = 2.4\times10^{-32}$, $\eta_p^2 = 0.011$).

Next associations between obesity groups were performed for individual cerebral GM regions. After adjustment for global GM volume, significant associations remained with the following regions: bilateral thalamus, bilateral caudate, bilateral pallidum, bilateral nucleus accumbens, after accounting for Bonferroni-corrected p-value of 0.004. Associations with bilateral putamen, bilateral amygdala, and bilateral hippocampus were not significant after Bonferroni correction (see Table 1).

Association with indicators of body-fat mass

(a) Bioelectrical impedance

Higher body-fat mass was associated with lower GM volume (see Fig 2), as well as lower total brain volume, but not with WM volume (see Table 2).

(b) Abdominal MRI

Higher total adipose tissue volume was associated with lower GM volume as well as lower total brain volume (see Table 3, Fig 3). By contrast, no association was found between total adipose tissue volume and WM volume (see Table 3).

(c) DXA

Fat-mass index (FMI) showed a significant negative effect on GM volume as well as total brain volume and but not on WM volume after adjusting for the covariates (see Supplementary Fig 2, Supplementary Table 1).

No association was found between network metrics and any indicator of body-fat mass irrespective of imaging modality

298

299 **Association with indicators of lean body mass**

300 **(a) Bioelectrical impedance**

301 Higher whole body-fat free mass was associated with lower GM volume, as well as
302 lower total brain volume (see Fig 2, Table 2). Similarly, a negative association was
303 found between whole body-fat free mass and WM volume (see Table 2).

304 **(b) Abdominal MRI**

305 Lean tissue volume (normalized by body weight) was not associated with any difference
306 in GM volume after adjusting for the covariates. Weak correlations were found between
307 total lean tissue volume (normalized by body weight) and normalized WM volume as
308 well as normalised total brain volume (see Table 3, Fig 3).

309 **(c) DXA**

310 Lean body-mass index (LBMI) showed a significant negative effect on GM volume as
311 well as total brain volume and but not on WM volume after adjusting for the covariates
312 (see Supplementary Fig 2, Supplementary Table 1).

313 No association was found between network metrics and any indicator of lean body mass
314 irrespective of imaging modality.

315

316 **Association with indicators of fat distribution**

317 **(a) Abdominal MRI**

Higher **visceral** adipose tissue volume was associated with lower total brain volume. As for WHR, this was explained by a significant negative correlation with GM volume after adjusting for covariates, before and after normalization by each subject's body weight ($p = 0.001$, Fig 3), but there was no association with WM volume (Table 3 and Fig 3).

Similarly, abdominal **subcutaneous** adipose tissue volume was negatively associated with GM volume and total brain volume (Table 3 and Fig 3). However, no significant correlation was found between abdominal subcutaneous adipose tissue volume and WM volume.

(b) DXA

Higher **visceral** adipose tissue mass was associated with lower GM volume and total brain volume, but not with WM volume or network metrics (Supplementary Table 1).

There was a significant negative correlation between android-to-gynoid fat ratio and GM volume before adjusting for the covariates ($r = -0.23$, $p = 1.3\times10^{-57}$), but this effect was not significant after adjusting for covariates ($r = 0.022$, 95% CI = [-0.01, 0.05]). Associations between android-to-gynoid fat ratio and WM volume were significant, but small in magnitude.

Trunk-to-leg fat mass ratio showed a significant negative correlation with GM volume before adjusting for the covariates ($r = -0.27$, $p = 8.3\times10^{-81}$, Fig 4). However, the trunk-to-leg fat mass ratio did not show a significant association with GM volume, total brain volume, or WM volume after adjusting for the covariates (Supplementary Table 1).

No association was found between network metrics and any indicator of fat distribution irrespective of imaging modality.

Association with cognitive scores

Analysis of co-variance did not reveal any significant effects of combined BMI/WHR group on the following cognitive scores: log-transformed number of incorrect matches in the visual memory task ($p = 0.313$), log-transformed difference between Trail making test – Part B and Trail making test – Part A ($p = 0.388$), the prospective memory task score ($p = 0.756$), and the number of correctly made symbol digit matches ($p = 0.891$). The effect of combined BMI/WHR on the log-transformed, average time to correctly identify matches was not significant after correcting for multiple comparisons (uncorrected $p = 0.001$).

Mediation analysis using structural equation modelling

The effect of WHR on GM volume was not mediated by blood glucose, glycated haemoglobin (HbA1c), HDL cholesterol, systolic or diastolic blood pressure (all $p > 0.05$, Supplementary Fig 3-4). Similarly, the effects of visceral adipose tissue volume from abdominal MRI and visceral adipose tissue mass from dual X-ray absorptiometry were not mediated by any of the aforementioned mediators (Supplementary Fig 5).

Interactions between indicators of obesity and sex

Finally, we investigated interaction effects between indicators of obesity and sex when predicting GM, WM, WMH and total brain volumes (supplementary table 2). We found significant interaction effects between sex and body fat mass, body fat-free mass (impedance), abdominal subcutaneous adipose tissue volume (abdominal MRI) as well as adipose tissue volume (abdominal MRI). By contrast, no interaction with gender was found for android-to-gynoid fat mass ratio, trunk-to-leg fat mass ratio, or trunk-to-leg lean mass ratio.

364

365

Discussion

In this large population-based study, central obesity was associated with lower GM volume, but not with WM volume or brain network integrity. We assessed central obesity using a variety of techniques including WHR, visceral adipose tissue from abdominal MRI, DXA, and bioelectrical impedance. Consistent results, with a selective association with GM volume, were found when central obesity was assessed by these diverse techniques. Furthermore, indicators of central obesity (e.g. WHR) were more informative than indicators of general obesity (e.g. BMI) in predicting brain volumes and being overweight alone, as measured using BMI, did not seem to have a detrimental effect on the brain.

Our findings add to the existing knowledge in a number of ways. Firstly, it is in a larger sample size than previous studies, including over 15000 individuals. Secondly, we used multiple complementary methods for assessing central obesity (BMI/WHR, abdominal MRI, dual-energy X-ray absorptiometry (DXA), and bioelectric whole-body impedance) which increases the robustness of the findings. Thirdly, we showed the associations with central obesity and brain structure were specific for grey matter, and was not present with white matter or with brain network connectivity; associations with network connectivity have not previously been assessed to our knowledge.

Increasing evidence suggests that obesity affects the CNS, and cognitive function including attention, executive function, decision making, and verbal learning (39). Meta-analyses have shown strong associations between obesity, Alzheimer's disease, and other dementias, with obesity in midlife predicting future dementia risk (2,40). Postmortem studies have shown that elderly individuals with morbid obesity have

increased beta-amyloid and tau protein in the hippocampus and decreased hippocampal volume (41). However, how obesity links to impaired cognitive function and dementia remains uncertain. Previous studies, many in relatively small sample sizes, have shown associations between obesity and GM volume, but inconsistent associations with WM volume and WM ultrastructural function determined on DTI (4–6)

However, many of these have merely measured BMI as an estimate of obesity and have not looked at the fat distribution within the body. In central obesity, there is increased fat in the abdomen and internal organs that causes low-grade inflammation (39). Central obesity has been associated with metabolic syndrome that includes dyslipidemia, decreased insulin sensitivity, hyperinsulinemia, hypoglycemia, and hypertension (12). Our results suggest that it is central obesity rather than peripheral obesity that is associated with CNS damage.

While previous smaller studies have associated obesity with GM loss, there have been conflicting associations reported with WM volume and structure (4–6). Since obesity has been associated with cognitive deficits including executive function (42), which itself depends on complex brain networks depending on WM integrity and connectivity, we hypothesized that brain network analysis may be affected in obesity. However, despite examining associations in almost 20 000 individuals we found no evidence of any alteration in WM volume or ultrastructure as measured by DTI and brain network efficiency. This suggests that CNS damage associated with central obesity is primarily focused on GM. This most likely represents neuronal loss rather than degeneration of tracts, because the cell bodies of neurons are found in the grey matter of the brain. Associations we have detected with GM volume might represent changes relatively early in the course of detrimental effects of central obesity on the brain, and as

413 individuals age, more widespread changes may be identified with secondary axonal
414 degeneration and WM changes. Longitudinal studies are required to determine if this is
415 indeed the case.

416 While central obesity, perhaps acting via the metabolic syndrome, may result in brain
417 atrophy, it is also possible that preexisting alterations in brain structure and function
418 play a causal role in obesity itself. Several neural circuits have been described which are
419 involved in energy balance and affect appetite and thermogenesis. Unconscious reward
420 circuits involve the striatum, amygdala, hippocampus, substantia nigra, hypothalamus
421 and brainstem which are all part of the dopaminergic mesocortical limbic circuit (39).
422 To determine whether there were specific regional associations with obesity we
423 examined associations with specific subcortical GM regions and the hippocampus. We
424 controlled for total GM volume to ensure that associations were region-specific. The
425 analysis identified specific associations with thalami, the caudate nuclei, pallidum, and
426 nuclei accumbens (all bilaterally). However, after controlling for multiple comparisons,
427 no association was found with the putamen, amygdala, or hippocampus. The caudate
428 nuclei, pallidum, and nuclei accumbens are known to play a key role in energy balance
429 that affect appetite, thermogenesis as well as inhibitory control (39). More specifically,
430 the nucleus accumbens is involved in components of reward-motivated behaviors (43)
431 as well as food addictions (36). The caudate nucleus and pallidum play a role in the
432 inhibitory control of eating (44) and contribute to physical inactivity in obesity (34).
433 Both the striatum and the nucleus accumbens (ventral striatum) are part of the
434 dopaminergic mesocortical limbic circuit that plays a crucial role in unconscious reward
435 (39) and has been suggested to be a common neurobiological circuit between food
436 addiction and drug abuse (36).

437 We explored potential pathways by which central obesity might result in GM atrophy
438 using mediation analysis. Central obesity has been associated with a low-grade
439 inflammatory state. However, the association between central obesity and GM volume
440 was not altered when C-reactive protein, a marker of systemic inflammation, was
441 controlled for. It has also been hypothesized that the metabolic syndrome may mediate
442 end-organ damage (45), but the associations of WHR, or visceral adipose tissue volume,
443 determined either on MRI or DEXA, was not mediated by blood glucose, HbA1c, HDL
444 cholesterol, systolic or diastolic blood pressure. This does not support a direct mediation
445 by individual features of the metabolic syndrome. Further studies are required to
446 determine which factors associated with central obesity mediate the association with
447 GM atrophy.

448 Central obesity might lead to neuronal loss or shrinkage of neurons in the cerebral GM
449 that is then not seen in the WM in the first place. Previous research on obesity in UK
450 Biobank found that higher total body fat was associated with lower subcortical GM
451 volumes, including the thalamus, caudate nucleus, putamen, globus pallidus,
452 hippocampus, and nucleus accumbens (46). These findings are similar to our results
453 when looking at the negative effect of WHR on the whole brain and subcortical GM
454 volume. A further UK Biobank paper showed that the combination of being overweight
455 according to BMI criteria and central obesity as indicated by WHR was associated with
456 lower GM volume, whereas no association between obesity and WM volume were
457 found (9).

458 Our study has several strengths. This includes a large sample size and the population-
459 based sampling framework. We estimated central obesity using multiple different
460 techniques and showed consistency of findings when central obesity was determined by

these different methods. This is important because each method has its limitations. DXA can be inaccurate in people with obesity. Impedance measures also depend on hydration levels. The body MRI data we were able to use only covered the abdomen rather than whole-body MRI and therefore an accurate estimate of whole-body fat could not be obtained. A further strength was that multiple methods were used to assess brain integrity, including not only conventional measures of GM and WM volume, but also DTI measures of network efficiency. The consistency of findings across WM measures adds robustness to the finding that WM structure does not appear to be altered in obesity.

Our study also has limitations. Its cross-sectional design means that we can identify associations but not causality. Although UK Biobank is a population-based study there is selection bias toward healthy volunteers. Lastly, although highly significant associations were identified, due to the very large sample size some of the effect sizes were small.

In conclusion, our results suggest that being overweight itself has only a limited effect on brain volume, but central obesity is associated with significant reductions in both global GM volume, and also with volume of specific subcortical GM nuclei.

Acknowledgements

This project was funded by the European Union's Horizon 2020 research and innovation programme [No 667375 (CoSTREAM)] with additional support from a BHF/Stroke Association programme grant (RG/16/4/32218). This research was conducted using the UK Biobank resource (application 36509). This work was supported by infrastructural support from the Cambridge University Hospitals Comprehensive Biomedical Research Centre. Hugh Markus and I. Sadaf Farooqi are supported by NIHR Senior Investigator awards.

Competing Interests

The authors have no competing interests to disclose.

Author contributions

CPP: analysis and interpretation of data, drafting or revising the manuscript for intellectual content

DJT: analysis and interpretation of data, drafting or revising the manuscript for intellectual content

ELH: analysis and interpretation of data, drafting or revising the manuscript for intellectual content

JT: analysis and interpretation of data, drafting or revising the manuscript for intellectual content

499 SF: drafting or revising the manuscript for intellectual content

500 HSM: drafting or revising the manuscript for intellectual content, obtained funding,
501 overall supervision.

References

1. Marcelin G, Silveira ALM, Martins LB, Ferreira AV, Clément K. Deciphering the cellular interplays underlying obesity-induced adipose tissue fibrosis. J Clin Invest. 2019 Oct;129(10):4032–40.

2. Pedditzi E, Peters R, Beckett N. The risk of overweight/obesity in mid-life and late life for the development of dementia: a systematic review and meta-analysis of longitudinal studies. Age Ageing. 2016 Jan;45(1):14–21.

3. Herrmann MJ, Tesar A-K, Beier J, Berg M, Warrings B. Grey matter alterations in obesity: A meta-analysis of whole-brain studies. Obes Rev an Off J Int Assoc Study Obes. 2019 Mar;20(3):464–71.

4. Yokum S, Ng J, Stice E. Relation of regional gray and white matter volumes to current BMI and future increases in BMI: a prospective MRI study. Int J Obes (Lond). 2012 May;36(5):656–64.

5. Walther K, Birdsill AC, Glisky EL, Ryan L. Structural brain differences and cognitive functioning related to body mass index in older females. Hum Brain Mapp. 2010 Jul;31(7):1052–64.

6. Haltia LT, Viljanen A, Parkkola R, Kemppainen N, Rinne JO, Nuutila P, et al. Brain white matter expansion in human obesity and the recovering effect of dieting. J Clin Endocrinol Metab. 2007 Aug;92(8):3278–84.

7. Vernooij M, Ikram M, Vrooman H, Wielopolski P, Krestin G, Hofman A, et al. White Matter Microstructural Integrity and Cognitive Function in a General Elderly Population. Arch Gen Psychiatry. 2009 Jun 1;66:545–53.

8. Zeestraten EA, Benjamin P, Lambert C, Lawrence AJ, Williams OA, Morris RG, et al. Application of Diffusion Tensor Imaging Parameters to Detect Change in Longitudinal Studies in Cerebral Small Vessel Disease. PLoS One [Internet]. 2016 Jan 25;11(1):e0147836. Available from: https://doi.org/10.1371/journal.pone.0147836

9. Hamer M, Batty GD. Association of body mass index and waist-to-hip ratio with brain structure: UK Biobank study. Neurology. 2019 Feb;92(6):e594–600.

10. Cameron AJ, Magliano DJ, Söderberg S. A systematic review of the impact of including both waist and hip circumference in risk models for cardiovascular diseases, diabetes and mortality. Obes Rev an Off J Int Assoc Study Obes. 2013 Jan;14(1):86–94.

11. Saklayen MG. The Global Epidemic of the Metabolic Syndrome. Curr Hypertens Rep [Internet]. 2018 Feb 26;20(2):12. Available from: https://www.ncbi.nlm.nih.gov/pubmed/29480368

12. Tune JD, Goodwill AG, Sassoon DJ, Mather KJ. Cardiovascular consequences of metabolic syndrome. Transl Res. 2017 May;183:57–70.

13. Razay G, Vreugdenhil A, Wilcock G. Obesity, Abdominal Obesity and Alzheimer Disease. Dement Geriatr Cogn Disord [Internet]. 2006;22(2):173–6. Available from: https://www.karger.com/DOI/10.1159/000094586

14. Borga M, West J, Bell JD, Harvey NC, Romu T, Heymsfield SB, et al. Advanced body composition assessment: from body mass index to body composition profiling. J Investig Med [Internet]. 2018/03/25. 2018 Jun;66(5):1–9. Available from: https://www.ncbi.nlm.nih.gov/pubmed/29581385

15. Shepherd JA, Ng BK, Sommer MJ, Heymsfield SB. Body composition by DXA. Bone [Internet]. 2017/06/16. 2017 Nov;104:101–5. Available from: https://www.ncbi.nlm.nih.gov/pubmed/28625918

16. Debette S, Wolf C, Lambert J-C, Crivello F, Soumaré A, Zhu Y-C, et al. Abdominal obesity and lower gray matter volume: a Mendelian randomization study. Neurobiol Aging. 2014 Feb;35(2):378–86.

17. Sudlow C, Gallacher J, Allen N, Beral V, Burton P, Danesh J, et al. UK biobank: an open access resource for identifying the causes of a wide range of complex diseases of middle and old age. PLoS Med [Internet]. 2015 Mar 31;12(3):e1001779–e1001779. Available from: https://www.ncbi.nlm.nih.gov/pubmed/25826379

18. Alfaro-Almagro F, Jenkinson M, Bangerter NK, Andersson JLR, Griffanti L, Douaud G, et al. Image processing and Quality Control for the first 10,000 brain imaging datasets from UK Biobank. Neuroimage [Internet]. 2017/10/24. 2018 Feb 1;166:400–24. Available from: https://www.ncbi.nlm.nih.gov/pubmed/29079522

19. West J, Dahlqvist Leinhard O, Romu T, Collins R, Garratt S, Bell JD, et al. Feasibility of MR-Based Body Composition Analysis in Large Scale Population Studies. PLoS One [Internet]. 2016 Sep 23;11(9):e0163332. Available from: https://doi.org/10.1371/journal.pone.0163332

20. Zhang Y, Brady M, Smith S. Segmentation of brain MR images through a hidden Markov random field model and the expectation-maximization algorithm. IEEE Trans Med Imaging. 2001 Jan;20(1):45–57.

21. Griffanti L, Zamboni G, Khan A, Li L, Bonifacio G, Sundaresan V, et al. BIANCA (Brain Intensity AbNormality Classification Algorithm): A new tool for automated segmentation of white matter hyperintensities. Neuroimage [Internet]. 2016;141:191–205. Available from: http://www.sciencedirect.com/science/article/pii/S1053811916303251

22. Shen J, Tozer DJ, Markus HS, Tay J. Network Efficiency Mediates the Relationship Between Vascular Burden and Cognitive Impairment: A Diffusion Tensor Imaging Study in UK Biobank. Stroke. 2020 Jun;51(6):1682–9.

23. Jenkinson M, Beckmann CF, Behrens TEJ, Woolrich MW, Smith SM. FSL. Neuroimage. 2012 Aug;62(2):782–90.

24. Tournier J-D, Calamante F, Connelly A. MRtrix: Diffusion tractography in crossing fiber regions. Int J Imaging Syst Technol [Internet]. 2012 Mar 1;22(1):53–66. Available from: https://doi.org/10.1002/ima.22005

25. Lawrence AJ, Tozer DJ, Stamatakis EA, Markus HS. A comparison of functional and tractography based networks in cerebral small vessel disease. NeuroImage Clin. 2018;18:425–32.

26. Tzourio-Mazoyer N, Landeau B, Papathanassiou D, Crivello F, Etard O, Delcroix N, et al. Automated Anatomical Labeling of Activations in SPM Using a Macroscopic Anatomical Parcellation of the MNI MRI Single-Subject Brain. Neuroimage [Internet]. 2002;15(1):273–89. Available from: http://www.sciencedirect.com/science/article/pii/S1053811901909784

27. Hagmann P, Kurant M, Gigandet X, Thiran P, Wedeen VJ, Meuli R, et al. Mapping human whole-brain structural networks with diffusion MRI. PLoS One

[Internet]. 2007 Jul 4;2(7):e597–e597. Available from: https://pubmed.ncbi.nlm.nih.gov/17611629

28. Latora V, Marchiori M. Efficient behavior of small-world networks. Phys Rev Lett. 2001 Nov;87(19):198701.

29. Latora V, Marchiori M. Economic small-world behavior in weighted networks. Eur Phys J B - Condens Matter Complex Syst [Internet]. 2003;32(2):249–63. Available from: https://doi.org/10.1140/epjb/e2003-00095-5

30. Watson CG, Stopp C, Newburger JW, Rivkin MJ. Graph theory analysis of cortical thickness networks in adolescents with d-transposition of the great arteries. Brain Behav [Internet]. 2018 Feb 1;8(2):e00834. Available from: https://doi.org/10.1002/brb3.834

31. Elliott P, Peakman TC. The UK Biobank sample handling and storage protocol for the collection, processing and archiving of human blood and urine. Int J Epidemiol. 2008 Apr;37(2):234–44.

32. McKinney W. {D}ata {S}tructures for {S}tatistical {C}omputing in {P}ython. In: van der Walt S, Millman J, editors. {P}roceedings of the 9th {P}ython in {S}cience {C}onference. 2010. p. 56–61.

33. Vallat R. Pingouin: statistics in Python. J Open Source Softw. 2018 Nov 19;3:1026.

34. Friend DM, Devarakonda K, O'Neal TJ, Skirzewski M, Papazoglou I, Kaplan AR, et al. Basal Ganglia Dysfunction Contributes to Physical Inactivity in Obesity. Cell Metab. 2017 Feb;25(2):312–21.

35. Bernardes G, IJzerman RG, Ten Kulve JS, Barkhof F, Diamant M, Veltman DJ, et al. Cortical and subcortical gray matter structural alterations in normoglycemic obese and type 2 diabetes patients: relationship with adiposity, glucose, and insulin. Metab Brain Dis. 2018 Aug;33(4):1211–22.

36. Lindgren E, Gray K, Miller G, Tyler R, Wiers CE, Volkow ND, et al. Food addiction: A common neurobiological mechanism with drug abuse. Front Biosci (Landmark Ed. 2018 Jan;23:811–36.

37. Oterdoom DLM, van Dijk G, Verhagen MHP, Jiawan VCR, Drost G, Emous M, et al. Therapeutic potential of deep brain stimulation of the nucleus accumbens in morbid obesity. Neurosurg Focus. 2018 Aug;45(2):E10.

38. Blunch N. Introduction to Structural Equation Modelling Using SPSS and AMOS [Internet]. London, England; 2008. Available from: https://methods.sagepub.com/book/intro-to-structural-equation-modelling-using-spss-amos

39. Devere R. The Cognitive Consequences of Obesity - Practical Neurology. Pract Neurol. 2018;

40. Anstey KJ, Cherbuin N, Budge M, Young J. Body mass index in midlife and late-life as a risk factor for dementia: a meta-analysis of prospective studies. Obes Rev an Off J Int Assoc Study Obes. 2011 May;12(5):e426-37.

41. Mrak RE. Alzheimer-type neuropathological changes in morbidly obese elderly individuals. Clin Neuropathol. 2009;28(1):40–5.

42. Yang Y, Shields GS, Guo C, Liu Y. Executive function performance in obesity

637 and overweight individuals: A meta-analysis and review. Neurosci Biobehav
638 Rev. 2018 Jan;84:225–44.

639 43. Castro DC, Berridge KC. Advances in the neurobiological bases for food “liking”
640 versus “wanting.” Physiol & Behav [Internet]. 2014 Sep;136:22—30.
641 Available from: https://europepmc.org/articles/PMC4246030

642 44. Bartholdy S, Dalton B, O’Daly OG, Campbell IC, Schmidt U. A systematic
643 review of the relationship between eating, weight and inhibitory control using
644 the stop signal task. Neurosci Biobehav Rev. 2016 May;64:35–62.

645 45. Alshehri AM. Metabolic syndrome and cardiovascular risk. J Family Community
646 Med. 2010 May;17(2):73–8.

647 46. Dekkers IA, Jansen PR, Lamb HJ. Obesity, Brain Volume, and White Matter
648 Microstructure at MRI: A Cross-sectional UK Biobank Study. Radiology. 2019
649 Jun;291(3):763–71.

650

651 **Figure Legends**

652 **Figure 1.** Association between BMI and WHR with GM and WM volumes, WMH and
653 brain network measures (global and local efficiency). Significant differences across the
654 stratified BMI and WHR groups are present for GM volume and WMH but not for WM
655 volumes or network measures. (Error bars show standard deviations, boxes correspond
656 to the interquartile range.)

657 **Figure 2** Scatter plots showing the significant negative effect of whole-body fat-free
658 mass and whole-body fat mass on the normalized cerebral GM volume. Pearson r in
659 these figures corresponds to the overall effect size of whole-body fat-free/fat mass on
660 cerebral GM volume **before** correction for the covariates.

661 **Figure 3**. Associations between indicators of body composition from abdominal MRI
662 and normalized GM volume. Visceral adipose tissue volume (normalized by body
663 weight), abdominal subcutaneous adipose tissue volume, total adipose tissue volume
664 and total lean tissue volume (normalized by body weight), derived from abdominal
665 MRI, as predictors of normalized cerebral GM volume. Pearson r in these figures
666 corresponds to the overall effect size of the association before correction for the
667 covariates.

668 **Tables**

669 **Table 1.** Analysis of covariance looking at the overall effect of the combined
670 BMI/WHR group on the volumes of subcortical regions-of-interest before and after
671 adjustment for total GM volume. P-values in bold are those significant after Bonferroni-
672 correction at p-value 0.004.

673 **Table 2.** Partial correlations between whole-body fat mass and whole-body fat-free
674 mass from bioelectrical impedance analysis and neuroimaging outcomes adjusted for
675 covariates.

676 **Table 3.** Partial correlations between indicators of body composition derived from
677 abdominal MRI and neuroimaging outcomes adjusted for covariates.

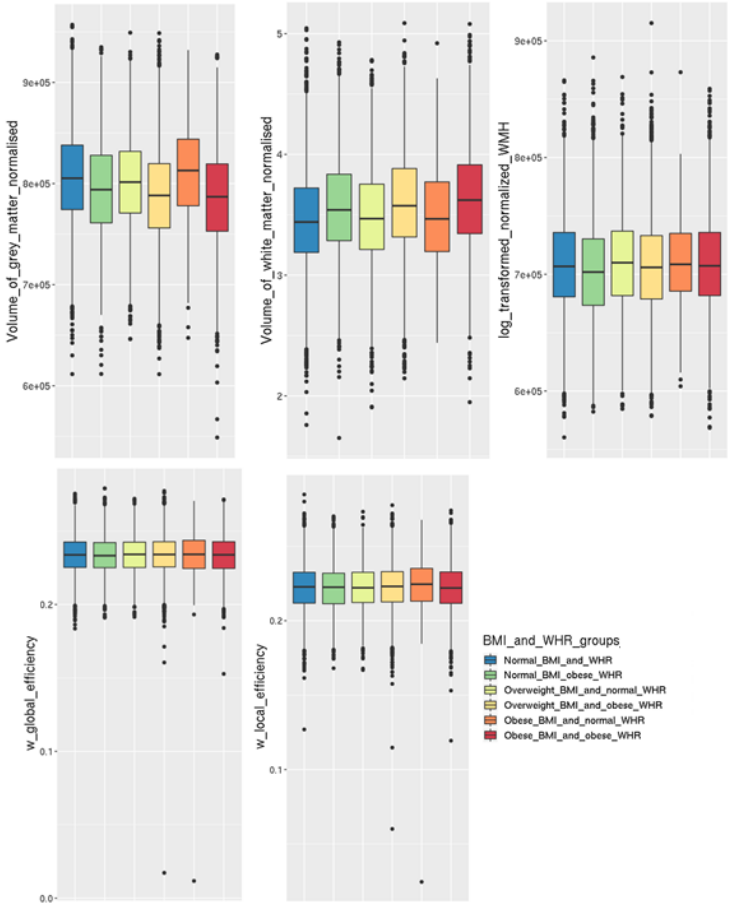
Volume_of_grey_matter_normalised
9e+05
8e+05
7e+05
6e+05
Volume_of_white_matter_normalised
5
4
3
2
log_transformed_normalized_WMH
9e+05
8e+05
7e+05
6e+05
w_global_efficiency
0.2
0.1
0.0
w_local_efficiency
0.2
0.1
BMI_and_WHR_groups
Normal_BMI_and_WHR
Normal_BMI_obese_WHR
Overweight_BMI_and_normal_WHR
Overweight_BMI_and_obese_WHR
Obese_BMI_and_normal_WHR
Obese_BMI_and_obese_WHR

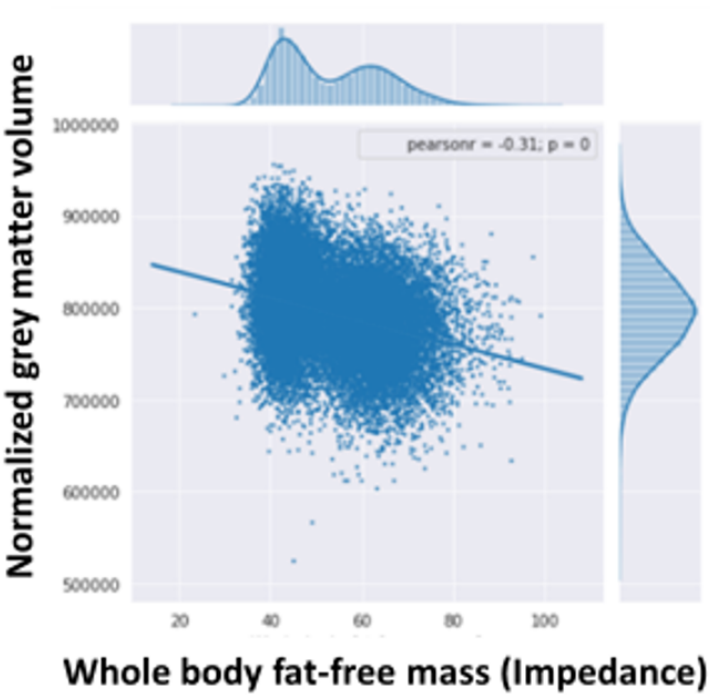
Normalized grey matter volume
pearsonr = -0.31; p = 0
1000000
900000
800000
700000
600000
500000
20
40
60
80
100
Whole body fat-free mass (Impedance)

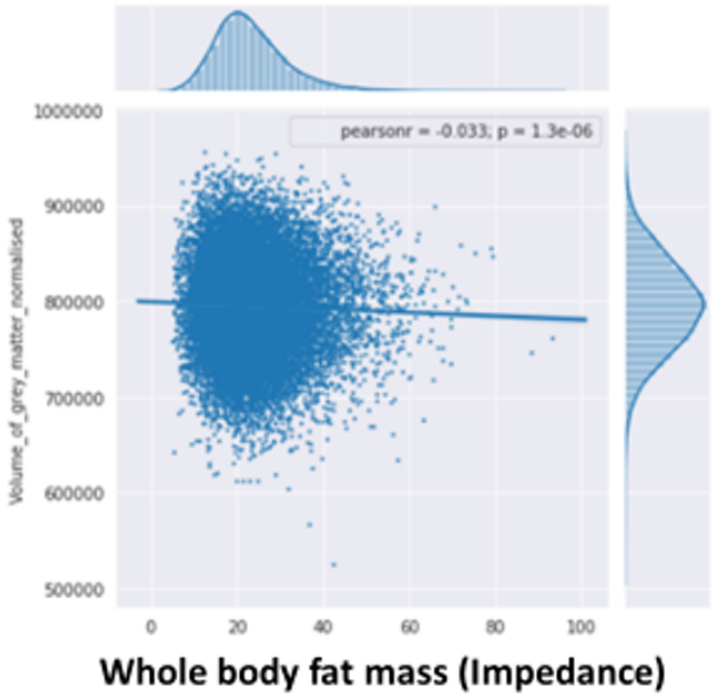
Volume_of_grey_matter_normalised
pearsonr = -0.033; p = 1.3e-06
1000000
900000
800000
700000
600000
500000
0
20
40
60
80
100
Whole body fat mass (Impedance)

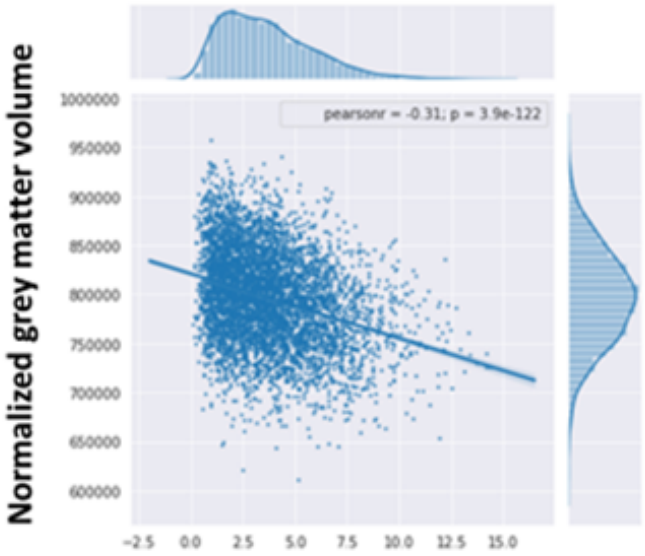

Visceral adipose tissue volume

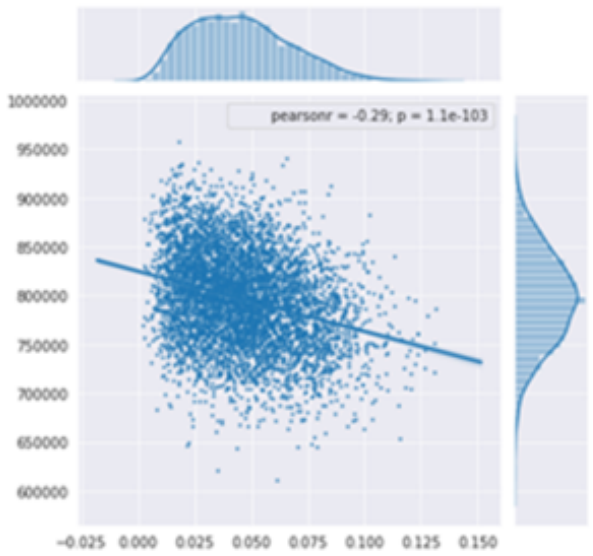

Visceral adipose tissue volume over body weight

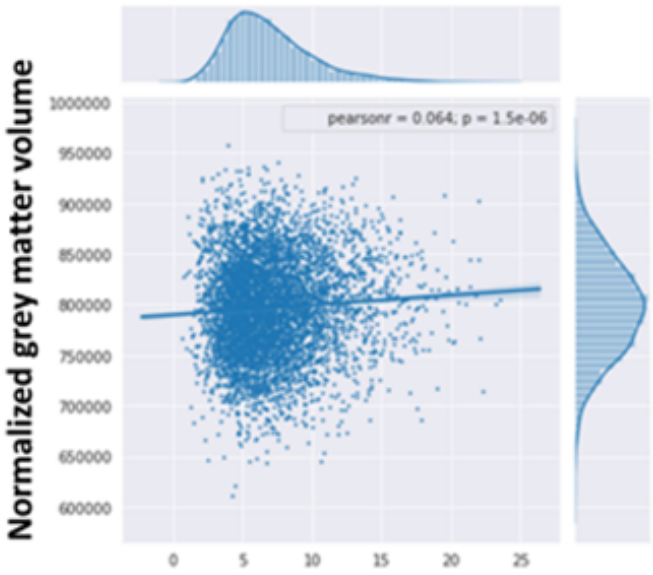

Abdominal subcutaneous adipose tissue volume

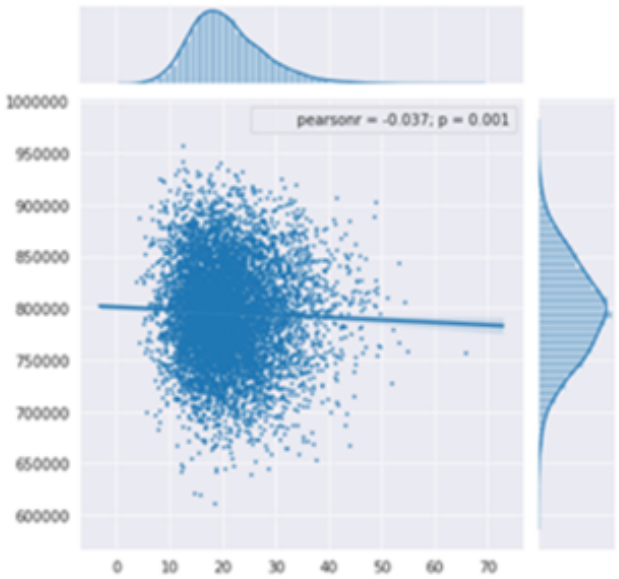

Total adipose tissue

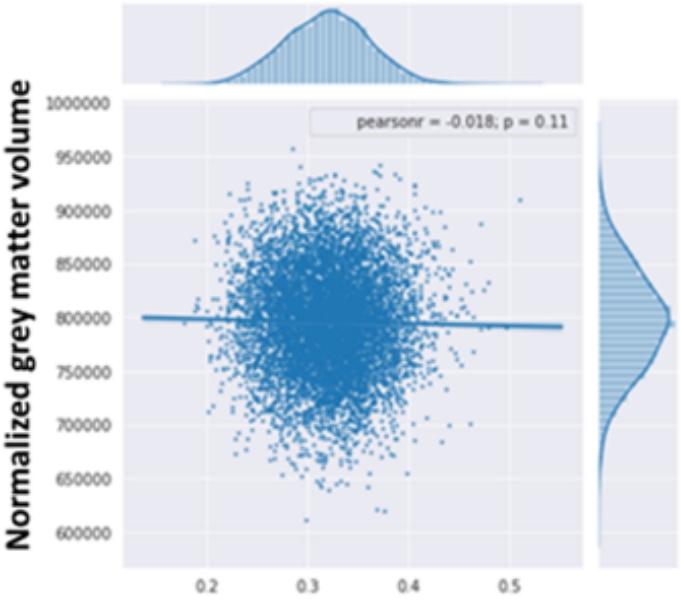

Total lean tissue volume over body weight

Region of interest	Hemisphere	Results adjusted for covariates				Results adju
		F (5, 15 619)	p-value	ηp2		F (5, 15 619)
Thalamus	left	**6.618**	**3.658 × 10-6**	**0.002**	*	**4.461**
Thalamus	right	**7.056**	**1.345 × 10-6**	**0.002**	*	**4.921**
Caudate	left	**5.98**	**1.559 × 10-5**	**0.001**	*	**5.235**
Caudate	right	**6.943**	**1.741 ×10-6**	**0.002**	*	**6.164**
Putamen	left	2.752	0.017	0.001		1.695
Putamen	right	2.668	0.02	8.542 × 10-4		1.478
Pallidum	left	**7.238**	**8.838 × 10-7**	**2.314 × 10-3**	*	**7.24**
Pallidum	right	**10.244**	**8.074 × 10-10**	**0.003**	*	**9.356**
Amygdala	left	2.751	0.017	8.81 ×10-4		2.733
Amygdala	right	**3.804**	**0.001**	**0.001**	*	**3.626**
Nucleus accumbens	left	**8.4318**	**5.606 × 10-8**	**0.002**	*	**4.886**
Nucleus accumbens	right	**9.884**	**1.882 × 10-9**	**0.003**	*	**5.676**
Hippocampus	left	0.927	0.461	2 × 10-3		0.586
Hippocampus	right	2.546	0.026	0.001		2.563

Table 1. Analysis of covariance looking at the overall effect of the combined BMI/WHR group on regions-of-interest before and after adjustment for total GM volume. P-values in bold are those sig p-value 0.004.

ısted for GM atrophy and covariates		
p-value	ηp2	
4.606×10-4	**0.001**	*
1.672×10-4	**0.001**	*
8.306×10-5	**0.001**	*
1.027×10-5	**0.002**	*
0.131	5.43×10-4	
0.193	0.0004	
8.798×10-7	**2.315×10-4**	*
6.489×10-9	**0.002**	*
0.018	0.001	
0.0028	**0.001**	*
1.805 ×10-4	**0.001**	*
3.098 ×10-5	**0.001**	*
0.071	1.88	
0.025	0.001	

ı the volumes of subcortical
nificant after Bonferroni-corretion at

Bioelectical impedance	Neuroimaging outcome	r	CI 95%	Adjusted variance explained
Whole body fat mass	**Brain volume**	**-0.071**	**[-0.09, -0.06]**	**0.005**
	GM volume	**-0.114**	**[-0.13, -0.1]**	**0.012**
	WM volume	-0.004	[-0.02, 0.01]	-0.0001
	Global Efficiency	0.001	[-0.01, 0.02]	-0.0001
	Local Efficiency	0.001	[-0.02, 0.02]	-0.0001
Whole body-fat free mass	**Brain volume**	**-0.121**	**[-0.14, -0.11]**	**0.014**
	GM volume	**-0.168**	**[-0.18, -0.15]**	**0.028**
	WM volume	-0.032	[-0.05, -0.02]	0.0009
	Global Efficiency	0.004	[-0.01, 0.02]	-0.0001
	Local Efficiency	0.003	[-0.01, 0.02]	-0.0001

Table 2. Partial correlations between whole-body fat mass and whole-body fat-free mass from bioelectrical impedance analysis and neuroimaging outcomes adjusted for covariates.

p-value	
1.772×10^{-19}	*****
2.925×10^{-47}	*****
0.533	
0.823	
0.887	
1.439×10^{-53}	*****
5.772×10^{-101}	*****
0.000037	*
0.588	
0.688	

Abdominal MRI	**Brain MRI**	r	CI 95%	Adjusted variance explained	p-value
visceral adipose tissue volume	**Brain volume**	**-0.072**	**[-0.1, -0.05]**	**0.00486**	**1.928×10^{-07}**
	GM volume	**-0.096**	**[-0.12, -0.07]**	**0.00888**	**4.279×10^{-12}**
	WM volume	0.023	[0.05, 0.0]	0.00018	0.085
	Global Efficiency	-0.011	[-0.02, 0.04]	0.00031	0.441
	Local Efficiency	-0.018	[-0.01, 0.05]	0.0001	0.217
abdominal subcutaneous adipose tissue volume	**Brain volume**	**-0.067**	**[-0.09, -0.04]**	**0.00419**	**0.000001**
	GM volume	**-0.094**	**[-0.12, -0.07]**	**0.0085**	**1.178×10^{-11}**
	WM volume	-0.018	[-0.05, 0.01]	0.00004	0.184
	Global Efficiency	0.015	[-0.01, 0.05]	0.00019	0.289
	Local Efficiency	0.01	[-0.02, 0.04]	0.00034	0.498
total adipose tissue volume	**Brain volume**	**-0.112**	**[-0.13, -0.09]**	**0.012**	**2.679×10^{-21}**
	GM volume	**-0.08**	**[-0.1, -0.06]**	**0.00614**	**1.157×10^{-11}**
	WM volume	-0.021	[-0.04, 0.0]	0.00016	0.075
	Global Efficiency	0.006	[-0.02, 0.03]	0.00028	0.649
	Local Efficiency	0.0003	[-0.02, 0.02]	0.0003	0.979
lean tissue volume (normalized by body weight)	**Brain volume**	**0.048**	**[0.03, 0.07]**	**0.002**	**0.00004**
	GM volume	**0.046**	**[0.02, 0.07]**	**0.001878**	**0.000093**
	WM volume	**0.032**	**[0.01, 0.06]**	**0.000762**	**0.0065**
	Global Efficiency	0.005	[-0.02, 0.03]	0.000283	0.649
	Local Efficiency	0.0003	[-0.02, 0.02]	0.000316	0.979

Table 3. Partial correlations between indicators of body composition derived from abdominal MRI and neuroimaging outcomes adjusted for covariates.

Significant
*
*
*
*
*
*
*
*
*